

(4), and (6). The guard plane half-width, d , is then determined by (5). After choosing k_d , then δ , $F(k', \delta)$, and $E(k', \delta)$ are obtained by (8), which now defines b , the strip half-width, from (7). Using (11), k_2 is readily found, from which $K(k_2)$, $K(k_2')$, and in turn C are determined.

Fig. 6 shows C , the capacitance of the strip-line per unit length, as a function of b , the half-width of the strip, for several values of d , the half-width of the ground planes. For values of b less than 1.00, the curves for d having values of 1.250 and infinity agree to about one-quarter of one per cent. The asymptotic values arise from exact expressions for the capacitance of parallel plate condensers.

It therefore follows that for $d > 1.25$ and $d > b + 0.25$, the exact capacitance and approximate value obtained by assuming infinite width ground planes agree within one-quarter of one per cent. A similar statement may be made for the characteristic impedance, since $R_0 = \sqrt{\mu_0 \epsilon_0 / C}$. The approximation is also valid for smaller values of d providing a more severe restriction is placed on the magnitude of b .

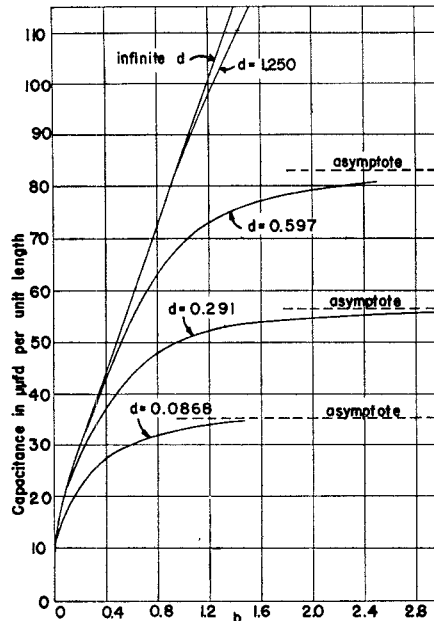


Fig. 6—Capacitance per unit length for a strip-line having a strip of width $2b$ centered between two ground planes each of width $2d$. The ground planes are separated by unit distance.

Resonant Frequencies of Higher-Order Modes in Radial Resonators

D. C. STINSON†

Summary—A summary of the relevant work on radial line discontinuities and radial line resonators is presented. A step-type discontinuity is analyzed using an integral equation formulation and the results are applied to the calculation of the resonant frequencies of a radial resonator. This method is verified by experiment and compared with the foreshortened-line approximation and with the methods of Marcuvitz and Goddard, whose work is satisfactory for the lowest-order TM mode. However, the present method is the only one which is equally applicable to the calculation of the resonant frequencies of TM modes possessing higher-order radial variations.

INTRODUCTION

RADIAL LINE discontinuities have been considered quite completely by Whinnery¹ and by Bracewell.² The former presents his data in the form of curves and takes into account such factors as the proximity of a shorting cylinder near the discontinuity and the effect of higher-order, nonpropagating modes. The latter treats only the simple step discontinuity, with the step facing either the inner region or the outer region, and takes into account radial variations by a cylindrical spread factor which is given by families of curves. These two papers form a very complete picture of radial line discontinuities.

Radial resonators have been considered by several approximate methods,³⁻⁵ but these ignore the discontinuity capacitance. Ordinarily, the discontinuity capacitance is of the same order of magnitude as the capacitance of the capacity loading of the gap, region A , in Fig. 1, if one considers the resonator as a foreshortened radial or coaxial line resonator. A better method considers the modes in both regions and matches them across the aperture, $r = a$. This method has been used

by F. E. Terman, "Radio Engineers' Handbook," McGraw-Hill Book Co., Inc., New York, N. Y., p. 268; 1943.

⁴ S. Ramo and J. R. Whinnery, "Fields and Waves in Modern Radio," John Wiley and Sons, Inc., New York, N. Y., pp. 404-412; 1944.

⁵ J. C. Slater, "Microwave Electronics," D. Van Nostrand Co., Inc., New York, N. Y., p. 234; 1950.

† Elect. Res. Lab., Univ. of Calif., Berkeley, Calif.

¹ J. R. Whinnery, "Radial line discontinuities," Elec. Lab., General Electric Co., D. F. #46293; June 22, 1944.

² J. R. Whinnery and D. C. Stinson, "Radial line discontinuities," PROC. IRE, vol. 43, pp. 46-51; January.

³ R. N. Bracewell, "Step discontinuities in disk transmission lines," PROC. IRE, vol. 42, pp. 1543-1548; October, 1954.

by Goddard⁶ and Marcuvitz⁷ and is exact until they introduce approximations for the discontinuity admittance and the Bessel functions.

However, the treatment of Marcuvitz and Goddard applies only to the lowest-order radial mode, i.e., TM_{010} mode. Their papers also include no experimental checks on the approximations involved. Further, the infinite-series method used by Goddard does not give results which are as easy to apply or as accurate as results obtained by using the integral-equation method, which he mentions but does not use. In the work to follow, the integral-equation method will be used to obtain the discontinuity capacitance of a radial line with a simple step and this result will then be applied to the calculation of the resonant frequencies of a radial resonator. Since the integral-equation method has been applied to many problems, the theoretical treatment will be very brief. A more detailed and rigorous treatment of this problem can be found elsewhere.⁸

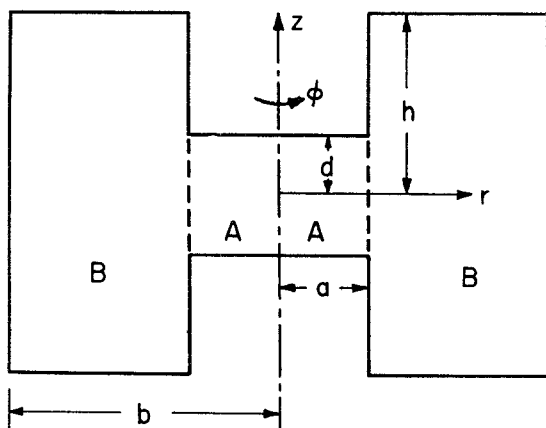


Fig. 1—Cross section of a radial resonator. Regions *A* and *B* are connected at the aperture, indicated by the dotted lines.

FORMULATION OF THE INTEGRAL EQUATIONS

The geometrical structure of the resonator dictates that the only nonvanishing field components in cylindrical co-ordinates be H_ϕ , E_z , E_r , the last being absent for the principal mode. The differential equations which govern the spatial behavior of H_ϕ , E_r , and E_z are

$$\begin{aligned} \left(\frac{\partial^2}{\partial r^2} + \frac{1}{r} \frac{\partial}{\partial r} + \frac{\partial^2}{\partial z^2} - \frac{1}{r^2} + k^2 \right) H_\phi(r, z) &= 0 \\ -j\omega\epsilon E_r(r, z) &= \frac{\partial}{\partial z} H_\phi(r, z) \\ i\omega\epsilon E_z(r, z) &= \left(\frac{\partial}{\partial r} + \frac{1}{r} \right) H_\phi(r, z), \end{aligned} \quad (1)$$

⁶ L. S. Goddard, "A method for computing the resonant wavelength of a type of cavity resonator," *Proc. Cambridge Phil. Soc.*, vol. 41, part 2, pp. 160-176; August, 1945.

⁷ C. G. Montgomery, R. H. Dicke, and E. M. Purcell, "Principles of Microwave Circuits," McGraw-Hill Book Co., Inc., New York, N. Y., ch. 8; 1948.

⁸ Elec. Res. Lab. Rep., Univ. of Calif., Series No. 60, Issue No. 105, December 15, 1953.

where $k = \omega(\mu\epsilon)^{1/2} = (2\pi/\lambda)$, ω = angular frequency, λ = free-space wavelength, μ = permeability of free space, ϵ = dielectric constant of free space, and $j = (-1)^{1/2}$. The principal mode results from (1) when the z dependence vanishes. Eqs. (1) must be solved subject to the following boundary conditions:

$$\begin{aligned} E_z &= 0 \quad \text{on} \quad r = a, \quad d \leq |z| \leq h \\ E_z &= 0 \quad \text{on} \quad r = b, \quad 0 \leq |z| \leq h \\ E_r &= 0 \quad \text{on} \quad |z| = d, \quad 0 \leq r \leq a \\ E_r &= 0 \quad \text{on} \quad |z| = h, \quad a \leq r \leq b. \end{aligned} \quad (2)$$

Also E_z and H_ϕ are continuous at

$$r = a, \quad 0 \leq |z| \leq d. \quad (3)$$

A continuous solution for the entire resonator is contingent upon equality of the respective tangential components of electric and magnetic field across the aperture between the two regions according to (3). This insures the continuity of the normal component, E_r . Tangential and normal refer to the space location of the field components relative to the direction of propagation of energy (radially outward). The scalar function H_ϕ at any point in either region can be expressed in terms of integrals involving E_z in the aperture. The continuity relation (3) results in an integral equation to determine the aperture field E_z , and thence the electromagnetic field everywhere in the resonator. Alternatively, we may express the scalar function E_z at any point in either region in terms of integrals involving H_ϕ in the aperture. The continuity relation (3) again gives an integral equation to determine the aperture field H_ϕ .

We may also introduce a principal-mode voltage and current in each region as follows: the voltage at any cross section in the resonator is defined as the negative line integral of E_z in the z direction while the current at any cross section is defined as the line integral of the principal-mode part of H_ϕ about the z axis. The functions thus defined satisfy the transmission line equations ordinarily given for radial transmission lines.⁷ The equations are not uniform since both the characteristic impedance and propagation constant are functions of the radius; nevertheless, they do make possible the introduction of an equivalent radial transmission line to represent the principal-mode voltage and current in each region and a lumped shunt admittance to represent the higher-order nonpropagating modes at the discontinuity between the two regions.

The solutions of (1) consistent with the boundary conditions (2) in the two regions are as follows:

Region A

$$\begin{aligned} H_\phi^A &= A_0 J_1(kr) + \sum_{m=1}^{\infty} A_m J_1(\lambda_m r) \alpha_m(z) \\ E_z^A &= \frac{1}{j\omega\epsilon} \left[A_0 k J_0(kr) + \sum_{m=1}^{\infty} A_m \lambda_m J_0(\lambda_m r) \alpha_m(z) \right] \end{aligned} \quad (4)$$

$$\begin{aligned}
\lambda_m &= m\pi K_m^A d^{-1} \\
K_m^A &= [(2d/m\lambda)^2 - 1]^{1/2} \\
\alpha_m(z) &= \cos(m\pi z d^{-1}) \\
V^A(r) &= - \int_{-d}^d E_z^A dz = -2kdA_0 J_0(kr)(j\omega\epsilon)^{-1} \\
I^{(A)r} &= 2\pi r A_0 J_1(kr).
\end{aligned}$$

Region B

$$\begin{aligned}
H_\phi^B &= B_0 Q_1(kr) + \sum_{n=1}^{\infty} B_n Q_1(\gamma_n r) \beta_n(z) \\
E_z^B &= \frac{1}{j\omega\epsilon} \left[B_0 k Q_0(kr) + \sum_{n=1}^{\infty} B_n \gamma_n Q_0(\gamma_n r) \beta_n(z) \right] \\
\gamma_n &= n\pi K_n^B h^{-1} \\
K_n^B &= [(2h/n\lambda)^2 - 1]^{1/2} \\
\beta_n(z) &= \cos(n\pi z h^{-1}) \\
Q_i(\gamma_n r) &= J_i(\gamma_n r) - J_0(\gamma_n b) N_i(\gamma_n r) N_0^{-1}(\gamma_n b) \\
Q_i(kr) &= J_i(kr) - J_0(kb) N_i(kr) N_0^{-1}(kb), \quad i = 0, 1. \\
V^B(r) &= - \int_{-h}^h E_z^B dz = -2khB_0(kr)(j\omega\epsilon)^{-1} \\
I^B(r) &= 2\pi r B_0 Q_1(kr).
\end{aligned} \tag{5}$$

We may now use the orthogonality properties of the circular functions to solve (4) and (5) for the coefficients A_m and B_n in terms of E_z . These coefficients are then substituted back into the expressions for H_ϕ^A and H_ϕ^B in (4) and (5) after replacing A_0 and B_0 by the corresponding expressions for the principal-mode currents. Now, since H_ϕ is continuous at the aperture according to (3), we may equate the expressions just derived and multiply by $2\pi a$ to obtain

$$\begin{aligned}
I^A + j2a\omega\epsilon \sum_{m=1}^{\infty} E_{0m} \int_{-d}^d \mathcal{E}(z') \alpha_m(z') \alpha_m(z) dz' \\
= I^B + j2a\epsilon\omega \sum_{n=1}^{\infty} D_{0n} \int_{-d}^d \mathcal{E}(z') \beta_n(z') \beta_n(z) dz', \\
r = a, 0 \leq |z| \leq d,
\end{aligned} \tag{6}$$

where

$$\begin{aligned}
\mathcal{E}(z) &= E_z^A(a, z) = E_z^B(a, z) \\
E_{0m} &= J_1(\lambda_m a) [K_m^A J_0(\lambda_m a)]^{-1} m^{-1} \\
D_{0n} &= Q_1(\gamma_n a) [K_n^B Q_0(\gamma_n a)]^{-1} n^{-1}.
\end{aligned}$$

Since E_z is continuous at $r=a$ from (3), it may be seen from the expressions for the voltages in (4) and (5) and the definition of $\mathcal{E}(z)$ that

$$V^A = V^B = V = - \int_{-d}^d \mathcal{E}(z) dz \quad \text{at } r = a.$$

Moreover, the discontinuity admittance⁹ is just the

⁹ Ramo and Whinnery, *op. cit.*, p. 375.

discontinuity current, $I^A - I^B$, divided by V .¹⁰ Consequently, we may construct a variational principle for the discontinuity admittance by multiplying the integral equation (6) by $\mathcal{E}(z)$, integrating over $(-d, d)$, and then dividing the resultant equation by $[\int_{-d}^d \mathcal{E}(z) dz]^2$. We obtain

$$\begin{aligned}
C_d = 2a\epsilon \left[\int_{-d}^d \mathcal{E}(z) dz \right]^{-2} \left\{ \sum_{m=1}^{\infty} E_{0m} \left[\int_{-d}^d \mathcal{E}(z) \alpha_m(z) dz \right]^2 \right. \\
\left. - \sum_{n=1}^{\infty} D_{0n} \left[\int_{-d}^d \mathcal{E}(z) \beta_n(z) dz \right]^2 \right\},
\end{aligned} \tag{7}$$

which expresses the discontinuity capacitance in terms of the aperture electric field $\mathcal{E}(z)$, which is homogeneous in $\mathcal{E}(z)$, and which is stationary with respect to the first variation of $\mathcal{E}(z)$ about its correct value determined by (6).

Let us now derive a similar expression for the discontinuity impedance in terms of the aperture magnetic field $\mathcal{H}(z)$. To do this we return to (4) and (5) and solve for A_m and B_n in terms of H_ϕ , and A_0 and B_0 in terms of the corresponding expressions for the principal-mode voltages. Since E_z is also continuous at the aperture according to (3), we may equate these expressions just derived and, after multiplying through by $2j\omega\epsilon d^2$, obtain

$$\begin{aligned}
- j\omega\epsilon d V + 2\pi \sum_{m=1}^{\infty} E_{0m}^{-1} \int_{-d}^d \mathcal{H}(z') \alpha_m(z') \alpha_m(z) dz' \\
= - j\omega\epsilon d V + 2\pi\delta^2 \sum_{n=1}^{\infty} D_{0n}^{-1} \int_{-d}^d \mathcal{H}(z') \beta_n(z') \beta_n(z) dz', \\
r = a, 0 \leq |z| \leq d,
\end{aligned} \tag{8a}$$

$$0 = - j\omega\epsilon d \delta V + 2\pi\delta^2 \sum_{n=1}^{\infty} D_{0n}^{-1} \int_{-h}^h \mathcal{H}(z') \beta_n(z') \beta_n(z) dz', \\
r = a, d \leq |z| \leq h,$$

$$\tag{8b}$$

where

$$\begin{aligned}
\mathcal{H}(z) &= H_\phi^A(a, z) = H_\phi^B(a, z), \\
\delta &= d/h,
\end{aligned}$$

and where (2) was used to obtain (8b). To derive our second variational principle, we multiply the expressions in (8) by $\mathcal{H}(z)$ and integrate each over its respective range of validity. Recognizing that

$$\begin{aligned}
\int_{-d}^d \mathcal{H}(z) dz &= dI^A(\pi a)^{-1} \\
\int_{-h}^h \mathcal{H}(z) dz &= hI^B(\pi a)^{-1}
\end{aligned}$$

and also noting that the expression resulting from (8b)

¹⁰ The voltages defined here are double those defined in reference 7 and, consequently, the discontinuity capacitance will be half that obtained in reference 7 since the currents are the same. Naturally, the resonant frequencies of the resonator of Fig. 1 will be the same as those of the resonator in reference 7 since the modes are the same.

is still equal to zero, we may add it to the expression resulting from (8a) and divide through by $[\int_{-d}^d \mathfrak{C}(z) dz]^2$ to obtain

$$-\frac{1}{2}V\mathfrak{J}^{-1} = \pi(j\omega\epsilon)^{-1}\mathfrak{J}^{-2}\mathfrak{B}$$

where

$$\begin{aligned}\mathfrak{J} &= d^{-1} \int_{-d}^d \mathfrak{C}(z) dz - h^{-1} \int_{-h}^h \mathfrak{C}(z) dz = (\pi a)^{-1}(I^A - I^B) \\ &= (\pi a)^{-1}VY_d \\ \mathfrak{B} &= h^{-2} \sum_{n=1}^{\infty} D_{0n}^{-1} \left[\int_{-h}^h \mathfrak{C}(z) \beta_n(z) dz \right]^2 \\ &\quad - d^{-2} \sum_{m=1}^{\infty} E_{0m}^{-1} \left[\int_{-d}^d \mathfrak{C}(z) \alpha_m(z) dz \right]^2.\end{aligned}$$

Thus we find that

$$C_d^{-1} = -2(a\epsilon)^{-1}\mathfrak{J}^{-2}\mathfrak{B}. \quad (9)$$

We have now derived the two desired variational principles, (7) and (9), for the discontinuity capacitance. If we substitute the true $\mathcal{E}(z)$ into (7) and the true $\mathfrak{C}(z)$ into (9), obtained from (6) and (8), respectively, both variational principles will yield the same value for C_d . However, the two values of C_d resulting from approximate $\mathcal{E}(z)$ and $\mathfrak{C}(z)$ will differ, but both will be close to the true C_d if the trial functions are chosen appropriately. The errors in C_d are of the order of magnitude of the squares of the errors in $\mathcal{E}(z)$ and $\mathfrak{C}(z)$. Since the stationary quantity is real, (7) will yield a value below the true one while (9) will yield a value above it.^{11,12} It may also be shown that the first variation of the discontinuity capacitance vanishes with the first variation of $\mathcal{E}(z)$ and $\mathfrak{C}(z)$, but the proof will be omitted here.

APPLICATION OF THE VARIATIONAL PRINCIPLES

At this point one would ordinarily assume $\mathcal{E}(z)$ as a Fourier cosine series in the interval $(-d, d)$ and obtain C_d from (7) in terms of the Fourier coefficients. Application of the variational principle would then reduce the expression for C_d to a simpler one. Similarly, $\mathfrak{C}(z)$ would be obtained in terms of the Fourier cosine series for $\mathcal{E}(z)$ and the resulting expression would be substituted into (9); again application of the variational principle would result in a simpler expression for C_d^{-1} . Since these simpler expressions are exact, approximations may be effected to any desired degree. However, for a first approximation, one might consider only the leading term in each of the expressions and thus avoid further calculations. If we do this, we find that when the aperture electric field is equal to a constant, G , (7) becomes

¹¹ H. Levine and C. H. Papas, "Theory of the circular diffraction antenna," *Jour. Appl. Phys.*, vol. 22, pp. 29-43; January, 1951.

¹² J. W. Miles, "The equivalent circuit for a plane discontinuity in a cylindrical wave guide," *Proc. IRE*, vol. 34, pp. 728-743; October, 1946.

$$C_d = -2a\epsilon\pi^{-2} \sum_{n=1}^{\infty} nD_{0n}s_{n0}(\delta), \quad (10)$$

where $s_{n0}(\delta) = n^{-3}\delta^{-2} \sin^2(n\pi\delta)$.

In order to evaluate C_d^{-1} using (9), we must deduce an appropriate expression for $\mathfrak{C}(z)$. We may do this by solving for H_ϕ^B in (5) in terms of $\mathcal{E}(z)$ and then let $r=a$ to obtain

$$\mathfrak{C}(z) = (2\pi a)^{-1}I^B + j\omega\epsilon\pi^{-1}G \sum_{n=1}^{\infty} D_{0n}b_{0n}\beta_n(z),$$

where $b_{0n} = 2h(n\pi)^{-1} \sin(n\pi\delta)$. We now insert this value of $\mathfrak{C}(z)$ into (9) and find that the expression for C_d^{-1} reduces to the following, provided one considers only the leading terms:

$$C_d^{-1} = -2(a\epsilon)^{-1}d^2 \left[\sum_{n=1}^{\infty} \sum_{p=1}^{\infty} D_{0n}b_{0n}b_{0p} \right]^{-1}$$

$$\text{or} \quad C_d = -2a\epsilon\pi^{-2} \sum_{n=1}^{\infty} nD_{0n}s_{n0}(\delta) - \frac{1}{2}a\epsilon d^{-2} \sum_{n=1}^{\infty} \sum_{\substack{p=1 \\ n \neq p}}^{\infty} D_{0n}b_{0n}b_{0p}. \quad (11)$$

It may be seen that C_d as given by (11) is larger than C_d as given by (10) by the term involving the double summation. Although this term is not as small as desirable, experimental evidence shows that the first term in (11) gives satisfactory results. Considering the first term then and simplifying it by separating the part containing the Bessel functions, we find that

$$C_d = \frac{2a\epsilon}{\pi^2} \left[S_0(\delta) - \sum_{n=1}^{\infty} (1 + nD_{0n}) s_{n0}(\delta) \right], \quad (12)$$

where $S_0(\delta) = \sum_{n=1}^{\infty} s_{n0}(\delta)$ is the lowest-order Hahn¹³ function. These functions have been considered quite thoroughly by Goddard,¹⁴ who defines a general class of functions that for low orders reduce to the Hahn functions. He also derives recurrence relations for his functions and tabulates the most common ones.

RESONANT FREQUENCIES

An electromagnetic system is considered resonant when the average electric and magnetic energies within the system are equal. Since by an energy theorem¹⁵ the total susceptance of an electromagnetic system is proportional to the difference between the average electric and magnetic energies stored in the system, it follows that a resonant frequency is one that causes the total susceptance to vanish. Let us consider the total susceptance of the resonator at the discontinuity. The susceptance looking in the direction of decreasing radius

¹³ W. C. Hahn, "A new method for the calculation of cavity resonators," *Jour. Appl. Phys.*, vol. 12, pp. 62-68; January, 1941.

¹⁴ L. S. Goddard, "On the summation of certain trigonometric series," *Proc. Cambridge Phil. Soc.*, vol. 41, part 2, pp. 145-161; August, 1945.

¹⁵ Montgomery, Dicke and Purcell, *op. cit.*, p. 135.

is just the input susceptance of the inner radial transmission line while the susceptance looking in the direction of increasing radius consists of the sum of the discontinuity susceptance and the input susceptance of the outer radial transmission line. However, we already have the resonance condition from the expression for \Im in (9) if we change the form slightly as below

$$Y_d = V^{-1}I^A + V^{-1}I^B = 0.$$

If we divide through by the characteristic admittance of region B , we can obtain the resonance equation in terms of relative admittances with the characteristic admittance of region B as the base. This form is much simpler to solve graphically since multiplying constants are kept to a minimum. Following these suggestions and using the values for the admittances from (12), (4) and (5), respectively, the resonance equation reduces to

$$Q_1(ka)Q_0^{-1}(ka) = \delta^{-1}J_1(ka)J_0^{-1}(ka) + 2kh\pi^{-3}S_0(\delta), \quad (13)$$

where the term in (12) involving D_{0n} has been dropped. If we multiply each side of (13) by $-j\pi ah^{-1}\epsilon^{1/2}\mu^{-1/2}$, then the first term is the admittance of the outer radial line, the second term is the negative admittance of the inner radial line, and the last term is the negative discontinuity admittance when one ignores radial variations. Since the only approximation in (13) is the one concerning radial variations of the discontinuity capacitance, (13) should be the simplest expression which is likely to yield reasonable results under general conditions. The disadvantage to using (13) lies in the fact that one must resort to a graphical solution, which in this case is done by plotting each term of (13) versus ka with the ratios b/a , d/h and h/a as parameters. This is illustrated in Fig. 2 for the radial TM_{010} mode in a resonator with $b/a = 2$. Since y^A and y^B both behave as periodic functions, the higher-order radial TM modes may be found in the same manner by continuing the curves to larger values of ka .

It is also interesting to note that the radial resonator may be considered as a transition between a coaxial and a cylindrical resonator, i.e., when $\delta = 0$ and $\delta = 1$, respectively. This follows directly from resonance equation (13) in the following manner. When δ is zero the relative admittance of region B , y^B , becomes infinite. Consequently, the poles of y^B give the resonant frequencies of the radial resonator when δ is zero. However, the poles of y^B are just the solutions of $J_0(ka)N_0(kb) - J_0(kb)N_0(ka) = 0$, which is the equation whose roots determine the resonant frequencies of a coaxial resonator¹⁶ sustaining TM modes possessing only radial variations. On the other hand, when δ approaches unity, the discontinuity capacitance vanishes and we are left with $y^B = y^A$, which reduces to the equation ordinarily given for the resonant frequencies of cylindrical TM_{0n0} modes.¹⁷

¹⁶ H. B. Dwight, "Table of roots for natural frequencies in coaxial type cavities," *Jour. Math. Phys.*, vol. 27, pp. 84-89; April, 1948.

¹⁷ Ramo and Whinnery, *op. cit.*, p. 337.

If one wishes a more accurate solution to the resonance equation (13), it is possible to use values for the discontinuity capacitance obtained from references 1 or 2. This has not been done here since (13) is sufficiently accurate for most purposes. In fact, as mentioned in the Introduction, most writers have assumed that all the dimensions of the resonator are small compared with wavelength and have used approximate forms of (13).

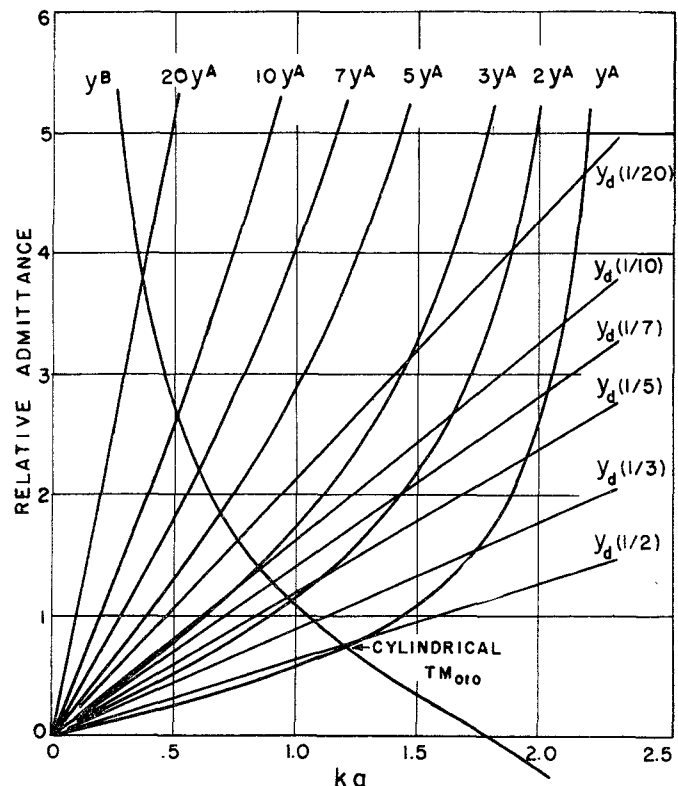


Fig. 2—Presentation of the resonance equation, $y^B(ka) = \delta^{-1}y^A(ka) + y_d(\delta)$, for the radial TM_{010} mode in the resonator of Fig. 1 with $b/a = 2$, where $k = 2\pi/\lambda$, λ = free-space wavelength and $\delta = d/h$.

The most simplifying assumption neglects the discontinuity capacitance entirely and uses small-argument approximations for the Bessel functions. This method considers the resonator as a foreshortened coaxial or radial resonator and permits one to solve for the resonant wavelength directly as

$$\lambda = \pi a [2\delta^{-1} \ln(r_1/r_0)]^{1/2},$$

which was done by Terman³ and Slater.⁵ A better approximation consists of using asymptotic expansions for the Bessel functions. This was done by Goddard,⁶ who was forced to solve an infinite set of simultaneous equations. Fortunately, the series for the coefficients of the system of equations converged very quickly, thus permitting a fairly rapid solution. A further approximation was used by Marcuvitz,⁷ who replaced the right side of (13) by $ka(2\delta)^{-1}$ and $2kh\pi^{-3}\ln(\frac{1}{4}e\delta^{-1})$, respectively, and then solved the resonance equation graphically by using curves of his radial functions. It should be noted that

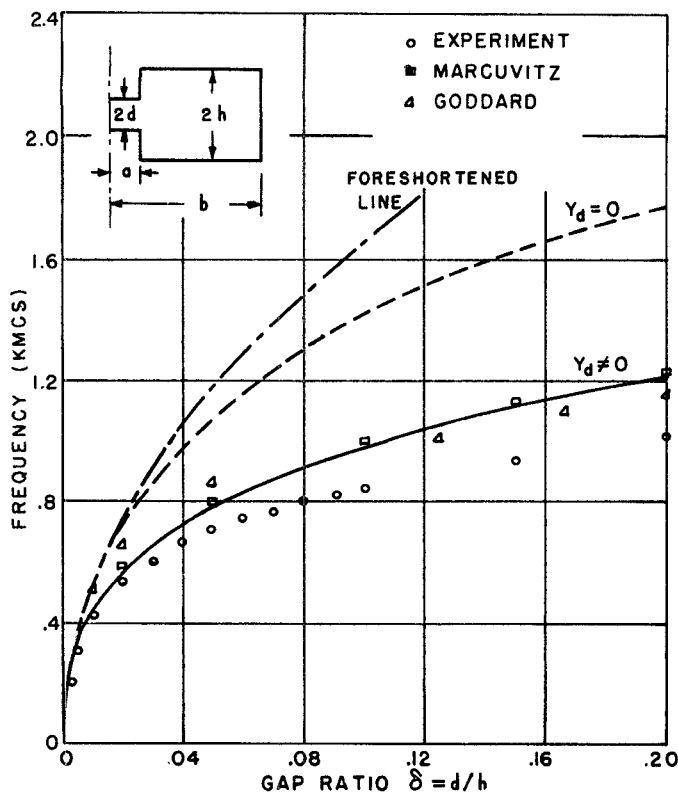


Fig. 3—Theoretical values of the resonant frequencies of radial TM_{010} mode for resonator of Fig. 1 with $b/a=5$, using methods of Marcuvitz and Goddard, and foreshortened-line approximation; compared with experiment and with values calculated using the integral-equation method when $Y_d=0$ and when $Y_d\neq 0$.

the left side of (13) is just the function which he defines as the small radial cotangent.

A comparison of the resonant frequencies obtained by using these different approximations with those obtained from (13) is given in Fig. 3 for a resonator with $b/a=5$. Fig. 3 also includes the solution of (13) when the discontinuity capacitance is ignored. Experimental values in this case are not too satisfactory since frequency effects in region B cause the approximation for the discontinuity capacitance to be poor. As mentioned in reference 1, the value for the discontinuity capacitance must be multiplied by a factor greater than unity when the value of h/λ becomes greater than about 0.2. This factor also becomes very large when h/λ approaches 0.5. For the resonator under consideration, the value of h/λ is about 0.22 when δ is 0.2.

Fig. 4 is another comparison of these approximate methods for a resonator with $b/a=2$. Experimental values in this case are reasonably close to the calculated ones considering the fact that h/λ is nearly 0.3 when δ is 0.5. Further experimental confirmation is given in Fig. 5, which is a set of comparison curves for a resonator with $b/a=6$. This figure also includes the radial TM_{020} mode, for which experimental values are quite good. Comparison curves for the radial TM_{030} and TM_{040} modes in the resonator of Fig. 4 and for the radial TM_{030} and TM_{040} modes in the resonator of Fig. 5 were obtained in reference 8 but are not shown here. However, the experimental errors for these higher-order modes were also

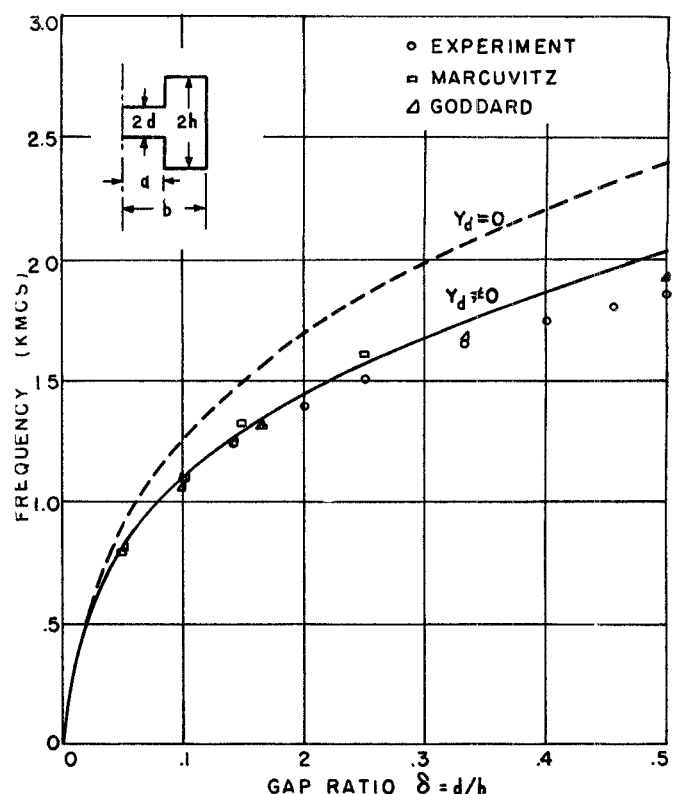


Fig. 4—Theoretical values of the resonant frequencies of the radial TM_{010} mode for the resonator of Fig. 1 with $b/a=2$ are shown using only the methods of Marcuvitz and Goddard. These are compared with values obtained from the integral-equation method and from experiment.

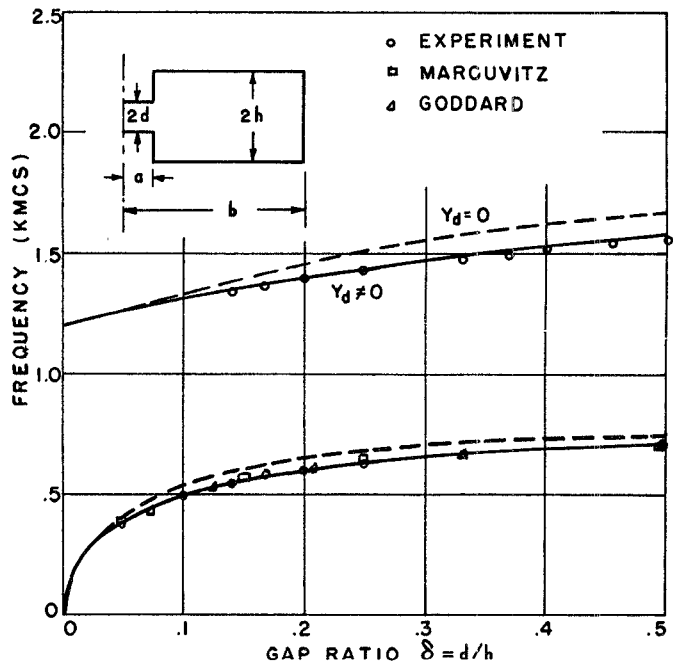


Fig. 5—Same as Fig. 4 but with $b/a=6$. The figure also includes the radial TM_{020} mode.

quite low. In all the cases we have considered, then, the approximations of Marcuvitz and Goddard are satisfactory for the lowest-order mode but give no information at all regarding the higher-order modes.